Colloid Polym Sci (2014) 292:1553–1565
DOI 10.1007/s00396-014-3215-y

ORIGINAL CONTRIBUTION

Charges of soluble amphiphiles and particles: random and diblock copolymerizations of MAA/AAm, MAA/St, and MAA/4VP in ethanol

Kan Zhan · Hui Zhang · Min Li · Yulu Chen · Guoxia Chen · Junxiu Liu · Min Wu · Henmei Ni

Received: 8 January 2014 / Revised: 18 March 2014 / Accepted: 28 March 2014 / Published online: 11 April 2014

Abstract Random and reversible addition-fragmentation chain transfer (RAFT) copolymerizations of methacrylic acid (MAA)/acrylamide (AAm), MAA/styrene (St), and MAA/4-vinyl pyridine (4VP) were carried out in ethanol. (CPDB)-terminated PMAA (PMAA-CPDB) and 2,2′-azobis (2,4-diemthylvaleronitrile) (V-65) was used as the macromolecular chain transfer agent (CTA) and initiator, respectively. Electric conductivity of copolymerization systems was traced throughout the polymerizations, and charges of soluble copolymer and particles were detected. As a result, a considerable increase of conductivity was observed in all of the RAFT polymerization systems, whereas the variation of conductivity in the random copolymerization systems was insignificant. The high conductivity of RAFT polymerization was dominantly contributed by the soluble diblock copolymers in the serum, rather than their particles, except for P(MAA-b-4VP) where only the particles was obtained due to the zwitterionic interactions of PMAA segments and 4VP. In the direct current (DC) field, the behavior of these soluble diblock copolymers, P(MAA-b-AAM) and P(MAA-b-St), indicated that they were positively charged, whereas the particles of (PMAA-b-AAm) and P(MAA-b-4VP) were surprisingly negatively charged, though the composition of MAA was dominant. Soluble random copolymers of P(MAA-co-St) and P(MAA-co-4VP) represented the charge neutrality. These results indicated that the positive charges were contributed by the solvophobic block in the soluble diblock copolymers. Therefore, the diblock copolymers were the macrodipoles boosting the conductivity of solution. Meanwhile, it indicated that the electrostatic interactions of dipoles were possibly the main driving force of their self-assembly. Generally, compared with RAFT polymerization, the particles were hard to be prepared in the random copolymerization. It implies that the electrostatic interactions of diblock copolymers also played an important role in the particle formation.

Keywords Electric conductivity · Amphiphilic diblock copolymer · Self-assembly · Poly(methacrylic acid)

K. Zhan · H. Zhang · M. Li · Y. Chen · G. Chen · J. Liu · M. Wu · H. Ni (✉)
School of Chemistry and Chemical Engineering, Southeast University, Southeast University Road 2, Jiangning Nanjing 211189, China
e-mail: Henmei_ni@hotmail.com

Introduction

Self-assembly of amphiphilic diblock copolymers to form spherical micelles, worms/rods, lamellae, toroids, vesicles, etc. is well known. The ordered polymeric nanostructures buildup the basis of soft nanotechnology and have presented many potential applications in different fields [1–4]. However, a limitation is obvious in the fabrication of nanostructures by self-assembly. For example, in order to control the self-assembly process, the formation of nanostructures is typically only conducted in a very dilute solution (<1 % solids), using processing techniques such as dialysis, a pH switch, or thin film rehydration [5–8]. Therefore, there is a strong interest in applying the principle of polymerization-induced self-assembly, i.e., create the nanostructures in situ and in a large scale, for the production of nanostructures. The conventional emulsion polymerization and dispersion/precipitation polymerization are the well-known approaches that both of them can produce the monodispersed nanoparticles in a large scale

[9, 10]. Hence, it is a good strategy to incorporate the synthetic approaches of diblock copolymers, e.g., ATRP, RAFT polymerization, etc. into the emulsion or precipitation copolymerization. Recently, a breakthrough has been made in this aspect, namely various nanostructures have been prepared by RAFT emulsion or dispersion/precipitation polymerizations [11–13]. For example, Charleux et al. have prepared the well-defined diblock copolymer micelles, worms, or vesicles by employing an efficient RAFT- and NMP-mediated aqueous emulsion polymerization [14–16]. Pan et al. have developed the RAFT nonaqueous precipitation polymerization to synthesize a wide range of nanostructures in alcohol by using polystyrene as a core-forming block combined with various alcohol-soluble stabilizer blocks [11, 17, 18]. Most recently, this method has been further developed to other core-forming polymerization systems [12, 19–21].

However, a mechanistic challenge arises from the great success in the preparation of nanostructures by using the conventional emulsion or dispersion/precipitation polymerizations. Mechanistically, the self-assembly process of amphiphilic diblock copolymers in selective solvents are considered as follows: (1) the insoluble components of macromolecules associate due to the hydrophobic or solvophobic interactions, giving rise to multichain aggregates; (2) the soluble components ensure the thermodynamic stability of the multichain aggregates in the solution. A typical example is a spherical micelle formed by diblock AB copolymer in a selective solvent. In such an aggregate, the micellar core composed of insoluble blocks B is surrounded by the corona of blocks A swollen by solvent, and the core-corona interface is narrow compared to the sizes of core and coronal domains. Based on this mechanism of self-assembly, two theoretical models have been proposed, i.e., the self-consistent field (SCF) methods and the scaling theory of polymer solutions [22, 23]. However, as we know, the polymerization methods such as the emulsion polymerization, precipitation/dispersion polymerization, etc., are conventional to both the industrial production of (co)polymers and the academic studies of the free-radical homopolymerization or random copolymerization. It is well known that in most cases the particles or microspheres are prepared by these methods [9, 10, 24–33]. In addition, the various morphologies of particles have been observed such as the common spheres [24–27], the half-spheres [28, 29], the dumbbell/egg-like particles [30], the hollow particles [31], the onion-like particles [32], etc. [33]. Mechanistically, these morphologies are considered to be the results of polymerization within the mini-/microdroplets of monomer preexisting in the systems of conventional emulsion or dispersion/precipitation polymerizations [9, 10]. That is to say, the precursor of hydrophobic or solvophobic core is originally a monomer droplet. Therefore, the difference is obvious. For example, in the random free-radical emulsion copolymerization of two monomers, the core-shell particles are often prepared where the polymer of relatively hydrophobic monomer forms the core [24, 30], whereas by the RAFT copolymerization, various morphologies may be prepared [4–21]. This difference is naturally considered to be resulted from the different structures of two copolymers, namely that by the RAFT copolymerization, the diblock copolymer is synthesized, whereas by the random copolymerization, the random copolymer is produced. Hence, it is necessary to investigate the properties of two copolymers.

Electric conductimetry is a common method to evaluate the amphiphilic behavior of surfactant and copolymer as well, for instance, the critical micellization concentration (CMC) of diblock copolymer [34]. The conductivity abruptly decreases as soon as the aggregation of diblock copolymers takes place since the free ions are hypothetically bound by the aggregations. Recently, this method has been developed to trace the particle formation in the soap-free emulsion polymerization of styrene [35] and the precipitation polymerization of MAA/AAm in ethanol [36, 37]. In these polymerization systems, however, it is observed that the conductivity abruptly increased as soon as the polymerization started, even though the water-insoluble initiators were used [35]. Moreover, even after the particles were born, the conductivity still continued to increase though the rate of increase declined. It is attributed to the soluble polymer or random copolymer generated in the continuous phase. According to the conventional mechanism of particle formation, the hydrophobicity of polystyrene increases as the chain grows [38]. At the critical length, the chains will precipitate from the continuous phase and then coagulate. Aforementioned above, this mechanism is also applied in the mechanistic explanation of self-assembly of diblock copolymer. Because the decrease of conductivity was not observed in the soap-free emulsion polymerization of styrene and the precipitation polymerization, a question is brought up, i.e., if it is possible for the polymer such as polystyrene in situ created in the continuous phase of soap-free emulsion polymerization to propagate to so long enough to aggregate. This question is also important for understanding the self-assembling behavior of diblock copolymer in situ generated in the RAFT precipitation polymerization. Therefore, the variation of conductivity provides the new information for elucidating the mechanism of particle formation and self-assembly of diblock copolymers.

In this paper, methacrylic acid (MAA) will be selected as the soluble component to copolymerize with acrylamide (AAm), styrene (St), and 4-vinyl pyridine (4VP) in ethanol. The features of these monomers are as follows: AAm is soluble in ethanol and interacts with both MAA and ethanol by hydrogen-bonds, but PAAm is solvophobic; PSt is only solvophobic; Both 4VP and P4VP are soluble in ethanol and interact with MAA. Electric conductivity of random and

RAFT copolymerization (PMAA as CTA) of MAA with these three monomers will be traced throughout the polymerization and charges of species in the copolymerization will be tested.

Experimental

Materials

All the chemical reagents used in this paper were purchased from Sinopharm Chemical Reagent Co. Ltd., Shanghai, China. Methacrylic acid (MAA), styrene (St), and 4-vinyl pyridine (4VP) were purified by distillation under the reduced pressure. Anhydrous ethanol was HPLC grade. The chain transfer agent (CTA), 4-cyanopentanoic acid dithiobenzoate (CPDB) (analytic grade), and the free-radical initiator, 2,2′-azobis(2,4-diemthylvaleronitrile) (V-65) (analytic grade) were used without further purification.

Polymerizations

All copolymerizations were performed in a four-necked 100-ml flask equipped with a thermometer, a condenser (also outlet of N_2), an inlet of N_2 gas, and an inlet for the insert of electric conductometer probe. The flask was settled in a thermostat water bath. V-65 was dissolved in ethanol and added into the polymerization system through the inlet of N_2 gas.

The formulated reagents except V-65 were added into the flask and deoxygenated by N_2 bubbling for 1 h at room temperature. After the temperature of water bath was elevated to 60 °C, V-65 ethanol solution was charged into the system. In order to control the variation range of initial conductivity, the amount of MAA or PMAA-CPDB was always kept at 1 wt%, while the amount of V-65 was constant at 2 wt% based on the total amount of monomers.

All of the final conversions of copolymerizations and RAFT polymerizations were more than 80 %.

PMAA-CPDB was prepared as follows: the molar ratio was MAA/CPDB/V–65=10,00/5/1 and the concentration of MAA was 25 wt% in ethanol. After all reagents were added into the flask, the system was deoxygenated by N_2 bubbling for 1 h at room temperature. The polymerization was carried out at 65 °C for 6 h. The transparent solution of polymerization system was turned into the pink viscous solution. Anhydrous ether was used to precipitate and wash the polymerization product. The product was characterized by ^{1}HNMR, Fourier transform infrared spectroscopy (FT-IR), and gel permeation chromatography (GPC). Figure 1 shows the spectra of CPDB and product. It was clear that, as shown in Fig. 1, PMAA-CPDB was successfully synthesized. The peaks of stretch vibrations of C═S (1,166 cm^{-1}) and C–S (697 cm^{-1}) in the FT-IR spectrum further confirmed that the product was PMAA-CPDB. The molecular weight of product measured by GPC were $\overline{M_w}$=7,000 and $\overline{M_n}$=6,080, respectively. PMAA-CPDB was dried in vacuum for 2 days and kept in a refrigerator (0 °C) before it was used.

Characterizations

A digital electric conductometer with the accuracy of ±0.001 μS (DDS-308A, Morechina Electronics Co. Ltd, Shanghai, China) was employed for the measurement of conductivity, while the polymerization systems were stirred by a magnetic stirrer. The conductivity of system was automatically on-line recorded (one data per 5 s) as soon as the deoxygenating N_2 bubbling started and throughout the successive polymerization. The scanning microscopy (SEM) (JSM-6360LV JEOL, Japan) and transmission electron microscopy (TEM) (Hitachi H-765, Hitachi Co. Ltd, Tokyo, Japan) images of particles were taken, which the preparation of samples was described elsewhere [9, 10]. A direct current (DC) power with the carbon electrodes was employed to setup DC field in the solution (maximum voltage 150 V, maximum currency 2 mA; type 1902; Shanghai Shengyuan Electronic Tech. Co. Ltd. Shanghai, China). The DC field was loaded by using voltage of 100 V and electric currency of 0 mA.

Results and discussion

Electric conductivity of random copolymerization and RAFT polymerization systems

Precipitation polymerization of MAA/AAm in alcohol has been well known as the polymerization system to prepare the pH-sensitive microgel. A lot of researches have been conducted in Kawaguchi's lab [25–27] and our lab [9, 36, 37]. However, recently the variation of conductivity in the polymerization process was traced for the first time [36, 37]. An amazing was observed that, as shown in Fig. 2, the conductivity of polymerization system of MAA/AAm abnormally and quickly increased after the polymerization started. Moreover, the increase rate of conductivity was always slow down as soon as the microgels were observable. In contrast, the conductivities of solution solely containing initiator, V-65, was almost constant at 60 °C for more than 300 min, though it decomposed. And also, the conductivity of MAA solution polymerization slightly increases as the polymerization progressed. Finally, AAm solution polymerization was special. The conductivity significantly decreased soon after the precipitation of PAAm coagulum. In our previous work [37], the conductivities of monomer solutions were detected at different concentrations and temperatures. In addition, the conductivity of PMAA ethanol solution with different concentration of AAm monomer was also measured. The considerable increase of conductivity was not

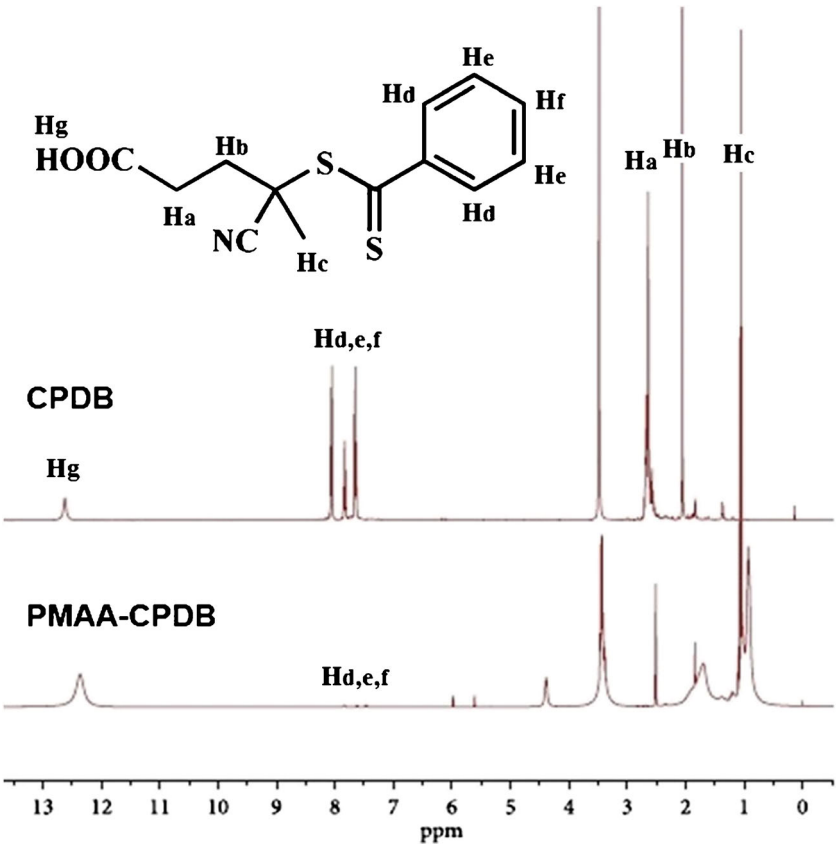

Fig. 1 ^{1}HNMR spectra of CPDB and PMAA-CPDB

observed in all of the systems. Hence, the results in present work indicated that the increase of conductivity was specific to the copolymerization systems of MAA/AAm, regardless to the dissociation constant of MAA or PMAA. Furthermore, the post-polymerization system of MAA/AAm was separated by the ultracentrifugation at 10,000 rpm. As shown in Fig. 3, the conductivities of serum were about 10.6 μS/cm at 25 °C and 17.8 μS/cm at 60 °C, whereas those of redispersed microgels were ca. 1.0 μS/cm at 25 °C and 1.5 μS/cm at 60 °C. All of the conductivities were constant for 120 min. It means that the conductivity stopped to increase when the copolymerization was completed. These results clearly indicated that, at first, the increase of conductivity was resulted from the species in situ generated in the copolymerization systems, rather than any foreigners or impurities coming from the surrounding. Secondly, the high conductivity was dominantly ascribed to

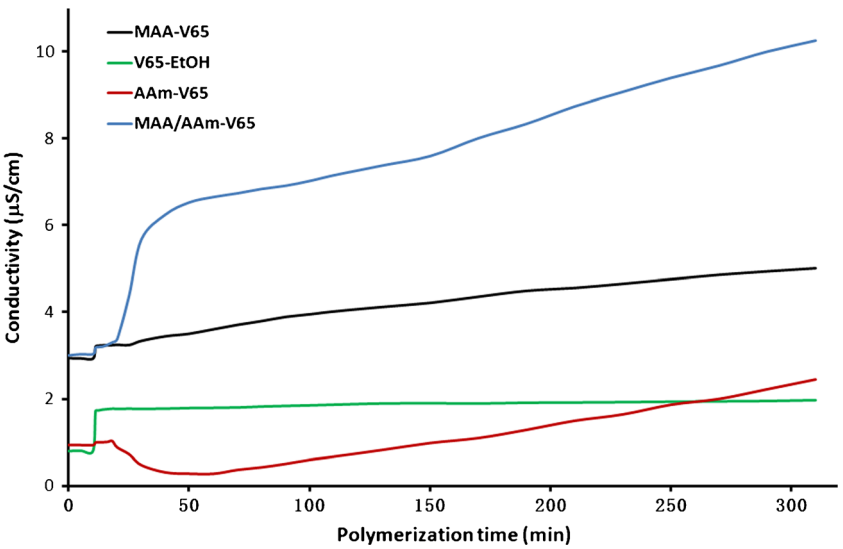

Fig. 2 Variation of conductivities of different polymerization systems

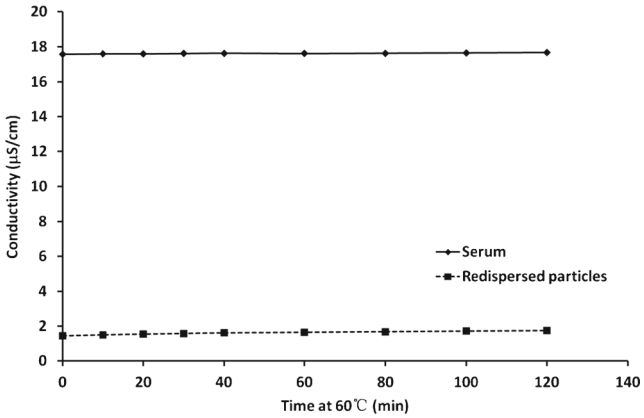

(a) Conductivity at 60 °C

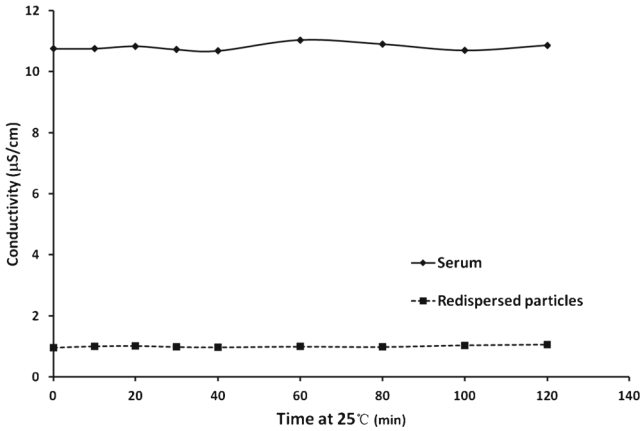

(b) Conductivity at 25 °C

Fig. 3 Conductivity of serum and the redispersed solution of PMAA/AAm particles. **a** Conductivity at 60 °C. **b** Conductivity at 25 °C

the species existing in the transparent serum. The transparent serum was further checked with the dynamic laser scattering (DLS), but no scattering object was observed. Therefore, it was concluded that the most of conductivity was contributed by the soluble copolymers of MAA/AAm, and a little was by the microgels.

In order to further confirm this result, the recipes of MAA/AAm copolymerization in ethanol were formulated deliberatively to circumvent the precipitation of copolymers, namely decreasing the amount of AAm to the utmost. As shown in Fig. 4, the molar ratio of MAA/AAm was changed from 10/1 to 80/1 while the total concentration of monomers was constant at 5 wt%. It should be noted that these solutions were the real solutions confirmed by DLS. When MAA/AAm was smaller than 10/1, for instance MAA/AAm=5/1, the resultant solution was slightly turbid indicating the precipitation of copolymers. It is clear that the conductivity increased as the copolymerization progressed. Moreover, with the increase of AAm, the conductivity increased. This result proved that the high conductivity of copolymerization system was did attribute to the soluble copolymers and the more AAm the higher

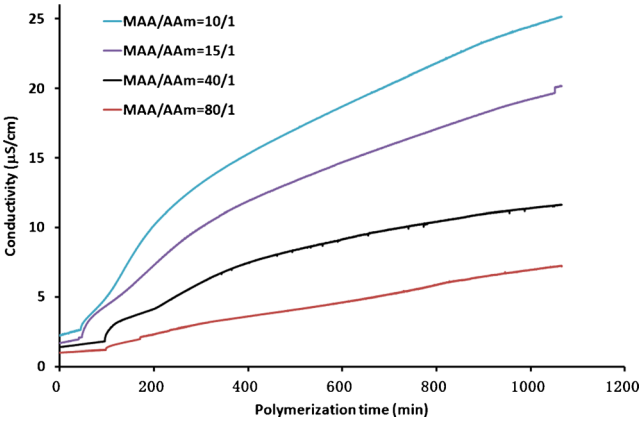

Fig. 4 Conductivity of copolymerization systems with a small amount of AAm

conductivity was obtained. It is well known that the reactivity ratios of copolymerization of MAA(1)/AAm(2) is disparate (r_1=1.63, r_2=0.57, Polymer Handbook). It is said that qualitatively the copolymer chains earlier formed contained less AAm units, while the later formed chains had more AAm units. It was the reason that the precipitation was observed though the amount of AAm was small, for instance, MAA/AAm=5/1. Nevertheless, this result implies that the increase of conductivity was likely related to the amount of AAm units in the soluble copolymer chains. Of course, the quantitative analysis needs the well-defined structure of copolymer chains. It was why the RAFT polymerization of AAm was carried out by using PMAA-CPDB as CTA, where PMAA-CPDB was constant at 1 wt%. As shown in Fig. 5, the variations of conductivity during the RAFT polymerization were similar to those in the random copolymerization (Fig. 4). For example, compared with the conductivity of MAA-CPDB and V-65 solution (Fig. 5a), the conductivity greatly increased when a

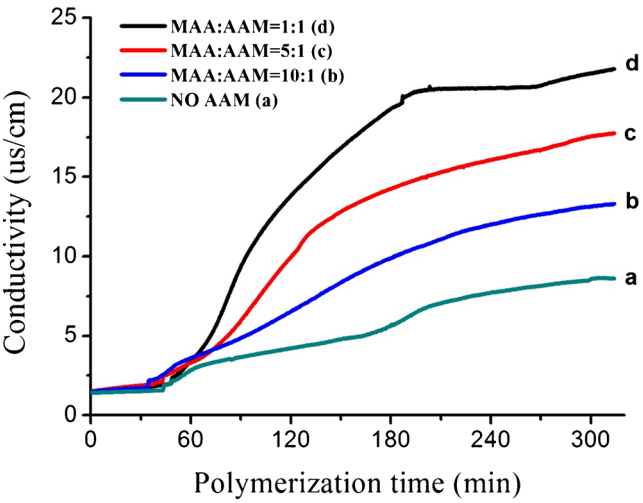

Fig. 5 Conductivity of RAFT polymerization of PMAA-CPDB/AAm. Curve (*a*) means the system of PMMA-CPDB and V-65 in the absence of AAm

little of AAm, e.g., MAA/AAm=10/1 (Fig. 5b), was added in the RAFT polymerization system. And also, the more AAm gave the higher conductivity. Additionally, when MAA units/AAm=1/1, a stage was observed on the curve (Fig. 5d), at which the conductivity ceased from increase but leveled off. This is a typical feature of conductivity variation of the polymerization systems where the stable microgels formed [36].

As we know, there are three kinds of species contributing to the conductivity, i.e., electron, ion, and colloidal particle or globule. In the above polymerization systems, only the ion was considerable because the conductivity was dominantly contributed by the soluble copolymer. Therefore, a reasonable resource of ions seems to come from MAA, namely that the dissociation of MAA releases H^+ and COO^-. Accordingly, AAm units in the copolymer seemed to promote the dissociation of MAA units. However, this explanation is not supported by the following experimental facts. For example, the random copolymerization of St(1)/AAm(2) (r_1=1.49, r_2=0.33), a similar system to that of MAA/AAm in ethanol, also gave rise to a dramatic increase of conductivity (not shown in this paper). PAAm is insoluble in alcohol, thus the diblock P(MAA-b-AAm) is a typical amphiphile where PMAA block is solvophilic and PAAm block is solvophobic. Therefore, the high conductivity was possibly ascribed to the structure of diblock. This proposition was strongly supported by the copolymerization systems of MAA/St.

The reactivity ratios of copolymerization indicate that the random copolymerization of MAA(1)/St(2) (r_1=0.38, r_2=0.28) tends to form the real random copolymer. Figures 6 and 7 show the conductivities of the random copolymerization of MAA/St and RAFT copolymerization of MAA (PMAA-CPDB)/St, respectively. As shown in Fig. 6, the variations of conductivity in the random copolymerization of MAA/St were insignificant compared with those of MAA and St homopolymerization systems. It indicated that the random copolymer of P(MAA-co-St) did not boost the conductivity. However, the conductivity was largely magnified in RAFT polymerization where the diblock copolymer of P(MAA-b-St) was produced (Fig. 7). P(MAA-b-St) is amphiphile in ethanol because PSt is insoluble. On the other hand, as shown in Fig. 7, the conductivity decreased as the amount of St increased from 10/1 to 1/5. It was different from that of MAA/AAm RAFT polymerizations. Here, it should be remarked previously that when MAA/St=1/2 and 1/5, the particles were prepared. At MAA/St=1/1, the system of RAFT polymerization was transparent at the polymerization temperature, 60 °C, but it changed into turbid at the room temperature. It indicated that P(MAA-b-St) was thermosensitive. It was precipitated at the lower temperature. This was possibly the reason that the conductivity decreased as the component of St increased in P(MAA-b-St).

As a comparison, the random and RAFT copolymerization of MAA/4VP were also conducted. In this copolymerization system, both the monomer and polymer are soluble in ethanol. A noticeable point was that MAA/4VP formed zwitterions. Therefore, it was normal that the conductivity increased as the amount of 4VP increased. However, as shown in Fig. 8a, in the random copolymerization, the conductivity was almost constant throughout the copolymerization, irrespective of the ratios. In contrast, the variation of conductivity was significant in RAFT polymerization systems. As shown in Fig. 8b, the conductivity greatly increased as soon as the polymerization started. The increment of conductivity related to the molar ratio of MAA/4VP. As MAA/4VP changed from 5/1 to 3/1, the final conductivity increased from ca 4 μS/cm to about 12 μS/cm, but as MAA/4VP further increased 1/1, the final conductivity decreased. On the other hand, an important result should be remarked that, in RAFT polymerization, the particles were prepared irrespective of the molar ratios, but in the random copolymerization, the particle was not obtained.

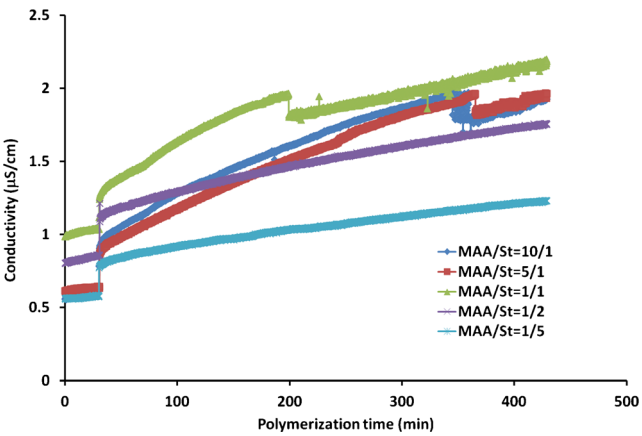

Fig. 6 Conductivity of random copolymerization of MAA/St

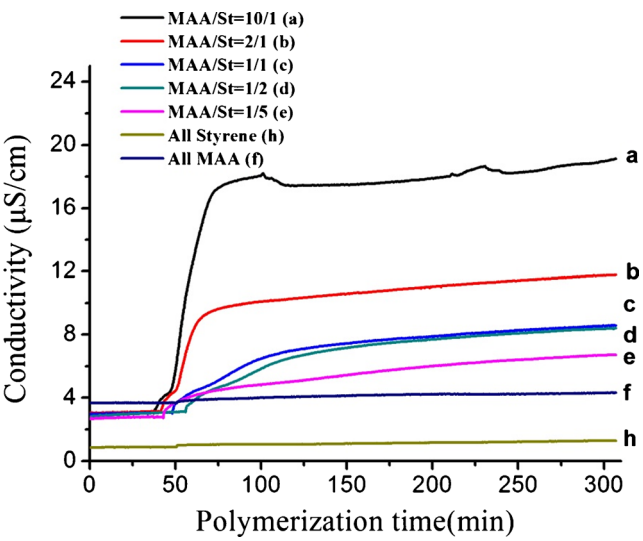

Fig. 7 Conductivity of RAFT copolymerization of PMAA-CPDB/St. Curve (*h*), the homopolymerization of St with V-65; curve (*f*), PMMA-CPDB, and V-65 in the absence of St

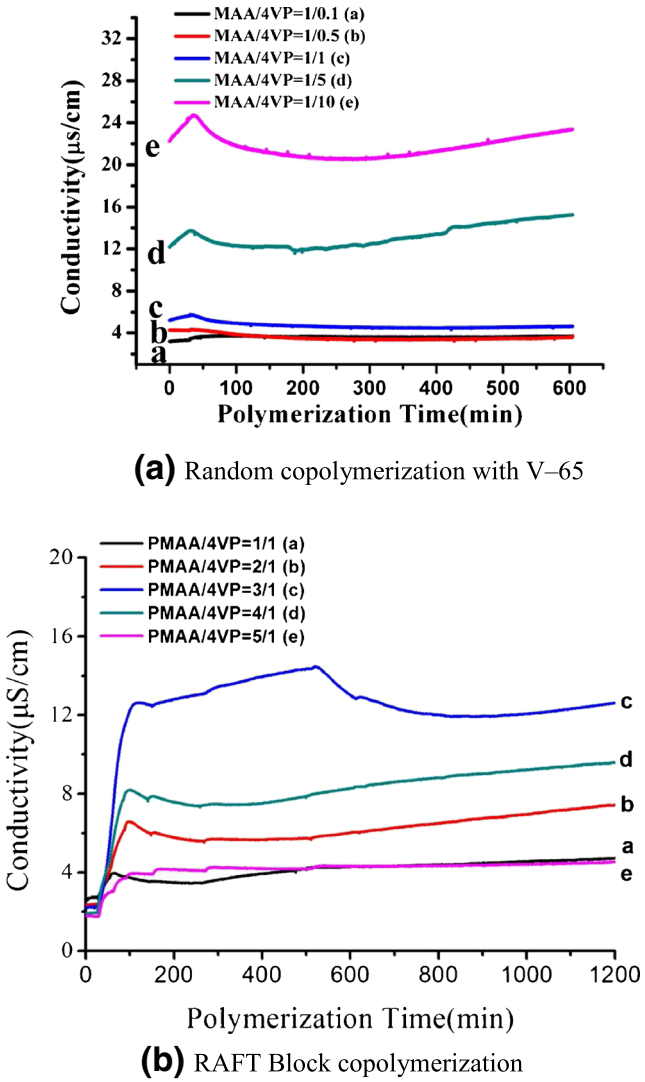

Fig. 8 Conductivity of RAFT copolymerization of PMAA-CPDB/4VP. **a** Random copolymerization with V-65. **b** RAFT block copolymerization

All these results indicated that the soluble diblock copolymer boosted the conductivity of ethanol solution, regardless to the chemical nature of solvophobic block. Moreover, the particles were more easily prepared by RAFT polymerizations.

Charges of species generated in the copolymerization systems

In order to determine the charges of species, the copolymerization systems were placed in a DC field (100 V, 0 mA) with carbon electrodes. The results are summarized in Table 1. It was amazing that, as shown in Fig. 9, both the soluble poly(MAA-co-AAm) and poly(MAA-b-AAm) were deposited on the cathode, i.e., negative side of DC field, while the particles were on the anode or positive side of DC field. In addition, the deposition of soluble copolymers was reversible, namely when the DC field was unloaded, the deposited copolymers gradually dissolved. In contrast, the deposited particles were not redispersible spontaneously. It should be pointed out that a fact was hindered by the deposition of particles (Fig. 9b), i.e., when the particles were separated by the ultracentrifugation, the soluble copolymers in the serum were also deposited on the cathode. Moreover, the conductivity decreased as the deposition proceeded. These results indicated that the soluble copolymers were positively charged, but the particles were negatively charged. Furthermore, the negatively charged particles and the positively charged soluble copolymers simultaneously coexisted in a copolymerization system.

As for the copolymerization of MAA/St, as shown in Table 1, it was complicated. In the random copolymerization, when the molar ratios of MAA/St were in the range from 10/1 to 1/2, the copolymerization systems were transparent. Meanwhile, the soluble random copolymers of P(MAA-co-St) were not deposited on any electrode. When the ratios of MAA/St were 1/5 and 1/10, the copolymerization systems were turbid. As shown in Fig. 10a, the deposition was found on both cathode and anode. Further investigated by SEM, it was observed that on the anode, those were big particles (beads), while on the cathode, it was membrane of polymer. It is said, the beads were negatively charged, whereas the soluble species were positively charged. Because St was five- and 10-folds of MAA, it was imaginable that PSt segment should exist in the copolymer chain, besides of the random block. This result was coincident to that observed in the system of MAA/AAm.

Inversely, in RAFT polymerization, when the ratios of MAA/St were from 10/1 to 2/1, the systems were transparent. As shown in Fig. 11a (upper pictures), P(MAA-b-St) was reversibly deposited on the cathode, i.e., positively charged. When MAA/St=1/1, it was interesting that the system was transparent at the polymerization temperature, 60 °C but turbid at room temperature. This result indicated that P(MAA-b-St) of MAA/St=1/1 was thermosensitive and the self-assembly occurred at the room temperature. The SEM photo of particles formed by self-assembly was shown in Fig. 11a (bottom pictures). These positively charged particles were about 50 nm (Fig. 11a). However, when MAA/St=1/2 and 1/5, the particles were prepared. Moreover, these particles were the charge neutrality (Table 1). Furthermore, as shown in Fig. 11b, in contrast to the very small (ca. 50 nm) and relatively monodispersed particles formed by self-assembly (Fig. 11a, bottom pictures), the particles in situ prepared by RAFT polymerization were very big, ca. 1,000 nm and polydispersed.

An interesting result was observed in Table 1. The homopolymers of PMAA, PSt, and P4VP did not deposit on any electrode, namely that they were charge neutrality. However, adding a small amount of KCl, PMAA was deposited on the cathode. It indicated that the insoluble groups of−COOK exhibited the positive charge (PMAA coagulated at the higher

Table 1 Charges of species generated in the copolymerization systems

Substance	Negative side	Positive side
PMAA	N	N
P4VP	N	N
PSt	N	N
Poly(MAA-co-AAm) (MAA/AAm=10/1−80/1)	Deposition	N
Poly(MAA-co-AAm) (MAA/AAm=1/2)	N	Deposition
Poly(MAA-co-St) (MAA/St=10/1, 5/1, 1/1, 1/2)	N	N
Poly(MAA-co-St) (MAA/St=1/5, 1/10)	Deposition	Deposition
Poly(MAA-b-St) (MAA/St=10/1,2/1,1/1)	Deposition	N
Poly(MAA-b-St) (MAA/St=1/2,1/5)	N	N
Poly(MAA-co-4VP) (MAA/4VP=10/1)	Deposition	N
Poly(MAA-co-4VP) (MAA/4VP=2/1,1/1,1/5,1/10)	N	N
Poly(MAA-b-4VP) (MAA/4VP=5/1,4/1,3/1,2/1)	Deposition	N
Poly(MAA-b-4VP) (MAA/4VP=1/1)	N	Deposition
PMAA/KCl	Deposition	N
P4VP/KCl	N	N
Poly(MAA-co-St)/KCl (MAA/St=10/1−1/2)	Deposition	N
Poly(MAA-co-St)/KCl (MAA/St=1/5,1/10)	Deposition	Deposition
Poly(MAA-b-St) /KCl (MAA/St=10/1,2/1,1/1)	Deposition	N
Poly(MAA-b-St)/KCl (MAA/St=1/2,1/5)	Deposition	N
Poly(MAA-co-4VP)/KCl (MAA/4VP=10/1, 2/1)	Deposition	N
Poly(MAA-co-4VP)/KCl (MAA/4VP=1/1−1/10)	N	N

concentration of KCl). Similarly, the charge neutral particles of P(MAA-b-St) with MAA/St=1/2 and 1/5, respectively, were also deposited on the cathode when KCl was added. This result indicated that there were PMAA segments on the surface of particles. Combined the result of TEM image, i.e., the heterogeneous distribution of composition in the particles (Fig. 11b, MAA/St=1/5), it implies that the charge neutrality of particles was possibly ascribed to the heterogeneous distribution of composition.

Furthermore, a surprising phenomenon was observed in the random copolymerization systems with MAA/St=1/5 and 1/10 in the presence of KCl. As shown in Fig. 10b, the negatively charged beads in the absence of KCl moved to the anode. It was expected since there were PMAA segments on the surface of beads. However, the porous film was found on the cathode. Reminiscent of membrane on the anode in the absence of KCl (Fig. 10a, bottom pictures), this result seems to say that the charges of soluble P(MAA-co-St) copolymer

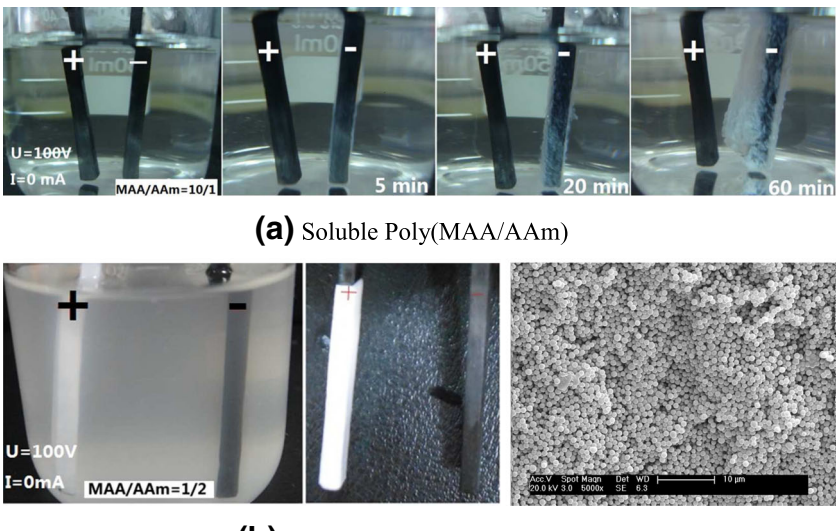

Fig. 9 Behavior of soluble P(MAA-co-AAm) and particles of P(MAA-co-AAm) in DC field. **a** Soluble poly(MAA/AAm). Random copolymerization system of MAA/AAm (10/1) (*left picture*); deposition of soluble poly(MAA-co-AAm) on cathode against time (*right pictures*). **b** Particles of poly(MAA/AAm). Random copolymerization system of MAA/AAm (3/1) (*left picture*); deposition of poly(MAA-co-AAm) particles on anode (*middle picture*) and SEM photo of poly(MAA-co-AAm) particles on anode (*right picture*)

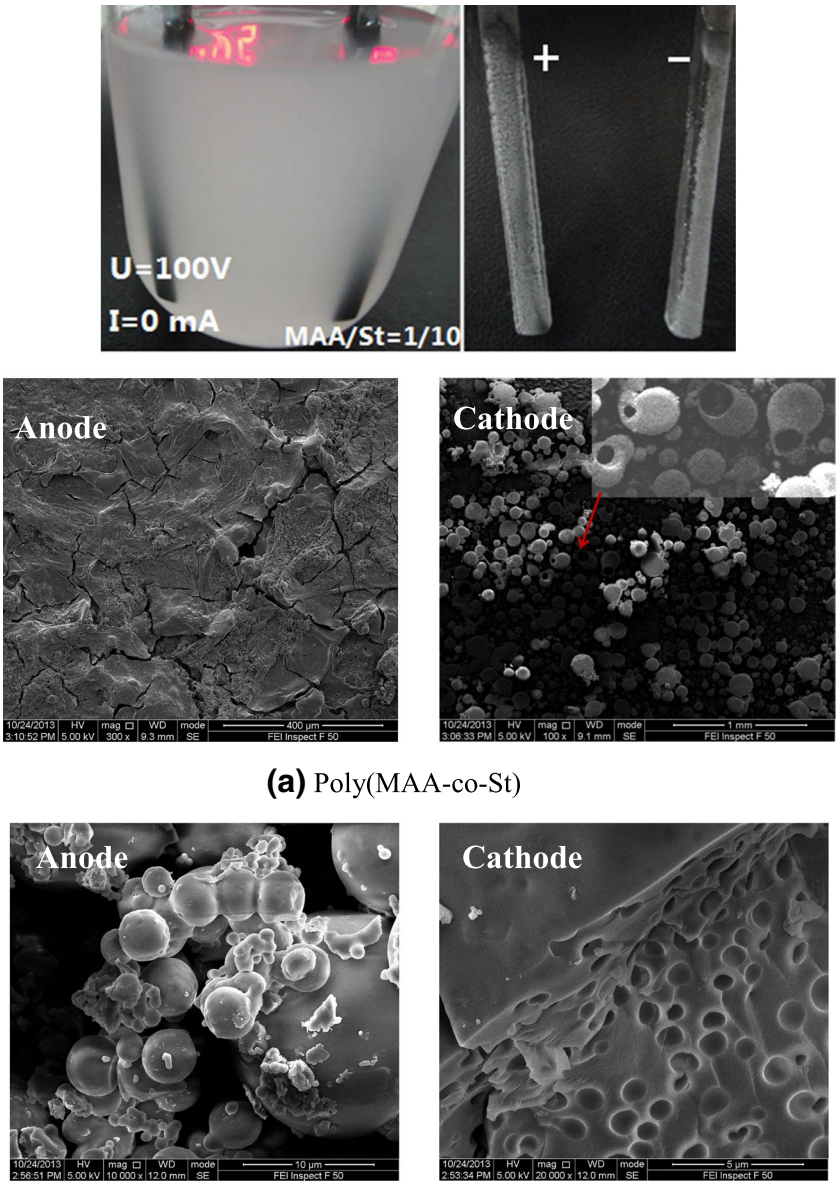

Fig. 10 Behavior of particles of random P(MAA-co-St) in DC field. **a** Poly(MAA-co-St). Random copolymerization system of MAA/St (1/5) (*upper*, *left picture*); Deposition of species on the anode and cathode (*upper*, *right picture*); SEM photos of species on the anode and cathode (*bottom pictures*). **b** Poly(MAA-co-St)/KCl. SEM photos of species on the anode and cathode which deposited in the solution of KCl/ethanol

were inverted by KCl, if assumed that the film was also made from the soluble copolymers. Moreover, as shown in Fig. 10a (bottom, right), b (right), the pores were always observed in the deposit of cathode, regardless to the presence of KCl. These pores, we think, were possibly the trace of monomer droplets, though it was arguable. It implies that the negatively charged monomer droplets were not changed by the addition of KCl.

As for the systems of MAA/4VP, it was very simple. In the random copolymerization systems, when the ratios of MAA/4VP were 10/1, 5/1 and 1/1, the cloudy precipitates were prepared. When MAA/4VP=1/5 and 1/10, the transparent gel was obtained. As shown in Table 1, the species in the random copolymerization systems did not deposit on any electrode, regardless to the molar ratios of MAA/4VP. These results were consistent with the constant conductivity of random copolymerization. However, in RAFT polymerizations, all species was deposited on the cathode, except for MAA/4VP=1/1 which deposited on the anode (Table 1). This result indicated that, when the amount of 4VP was less than that of MAA, the species was positively charged, whereas MAA=4VP, the species was negatively charged. In fact, as shown Fig. 12, in the RAFT polymerization systems, the species were all particles irrespective of the molar ratios. Moreover, the particle size decreased as the content of 4VP increased. The soluble block copolymer of poly(MAA-b-4VP) was not observed. It seems rational that the individual copolymer chain was hard to exist due to the strong isotropic interactions

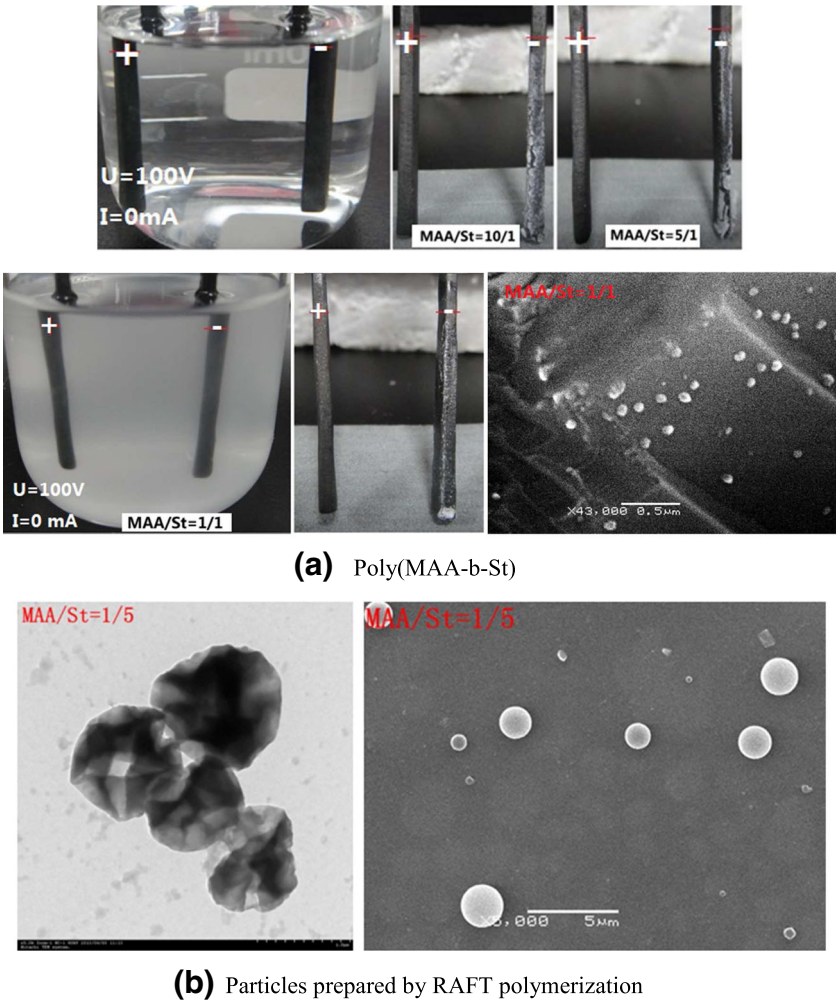

Fig. 11 Behavior of soluble P(MAA-b-St) and particles of P(MAA-b-St) in DC field. **a** Poly(MAA-b-St). *Upper pictures* indicate that the solutions of RAFT copolymerization of MAA/St (10/1 and 5/1) are transparent (*left picture*) and the deposition of the copolymers is on the cathode (*middle* and *right pictures*). *Bottom pictures* indicate that the self-assembly of block copolymer of MAA/St (1/1) at the room temperature (*left picture*), the self-assembled species deposited on the cathode (*middle picture*) and SEM photo of self-assembled species (*right picture*). **b** Particles prepared by RAFT polymerization. TEM and SEM photos of particles of block copolymer (MAA/St=1/5)

of ions. These results indicated that the charges were ascribed to the particles, rather than the soluble poly(MAA-b-4VP). Thereby, the behavior of conductivity in RAFT polymerization (Fig. 8b) was understandable because the conductivity was dependent to both the density of surface charges and mobility of particles. However, it was amazing that when the amount of PMAA-CPDB was dominant, the charges of P(MAA-b-4VP) particles were dominated by 4VP.

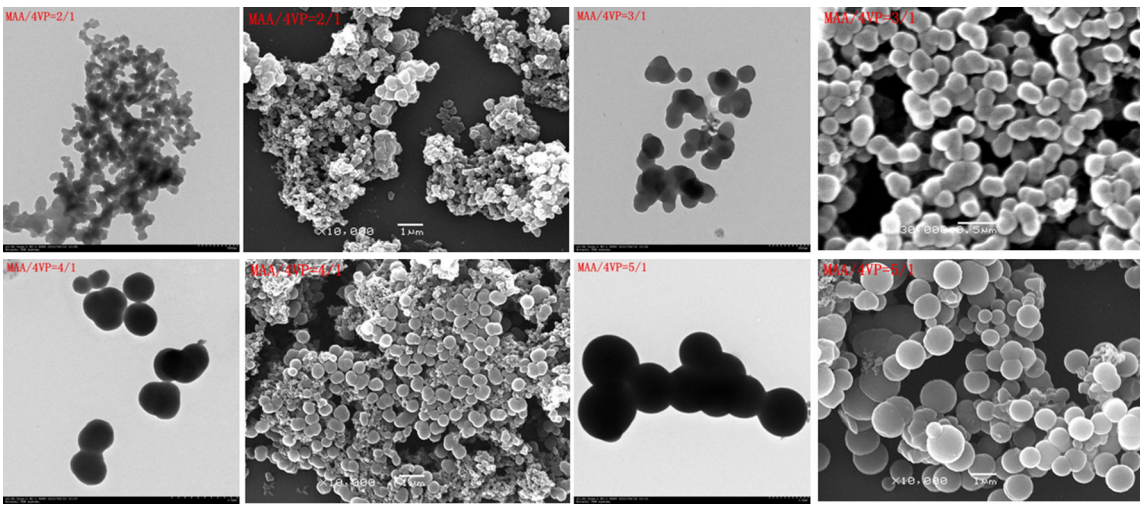

Fig. 12 SEM and TEM images of P(MAA-b-4VP)

According to the common knowledge, it is quite abnormal because 4VP is the donor of positive charge and MAA is the donor of negative charge.

Figure 12 also shows TEM images of species prepared. In contrast to the heterogeneous distribution of P(MAA-b-St) particles, it was observed that the distribution of composition in P(MAA-b-4VP) particles were homogeneous.

The positive charges indicated that the charge of soluble diblock copolymer was not ascribed to the donation of PMAA block. It was the specific nature of the soluble diblock amphiphile, i.e., the donation of solvophobic block regardless to the chemical nature of solvophobic block. This result was reminiscent of a conclusion in the studies of water interacting with interfaces, ions, and molecules. Based on the results of the dynamic behavior of hydrogen bond by ultrafast IR spectroscopy, it was concluded that water slowed the hydrogen bond dynamics substantially as evidence by changes in orientational relaxation times and chemical exchange dynamics [39]. When water interacted with an interface or a large molecule, the orientational relaxation time of water was slowed down to ~15–20 ps from that of its bulk, 2.6 ps. Furthermore, the presence of an interface was more important in slowing hydrogen bond dynamics than the chemical nature or geometry of the interface. In this paper, the interaction of hydrogen bond was common, for instance, ethanol interacted with MAA and AAm. Meanwhile, the generation of interface was imaginable because of the solvophobic block. More importantly, according to this conclusion, the result of charged poly(MAA-b-St) could be explained rationally. Namely, the birth of interface, rather than the chemical nature of interface, played the key role on slowing hydrogen bond dynamics. Accordingly, the solvophobic block was precipitated from the solution, thereby a new interface appeared, though the block copolymer was soluble entirely. The unbalanced orientational relaxation of ethanol hydrogen bond interacting with the solvophobic and solvophilic block of copolymer gave rise to the unbalanced charge distribution along the copolymer chain. It is a fact that, in the alcohol solution with the stronger hydrogen bond interaction, the soluble diblock copolymer gave rise to the higher conductivity. For example, the methanol solution of soluble poly(MAA/AAm) gave the highest conductivity among the methanol, ethanol and isopropanol solutions, while the conductivity of isopropanol solution was the lowest [36, 37]. Moreover, in the aqueous solution, the more hydrophobic species seemed to give the higher conductivity [35]. It was reported that when various water-insoluble initiators, i.e., azobis(isobutyronitrile) (AIBN), 2,2′-azobis(2-methyl-butyronitrile) (V-59), poly(ethylene glycol)-azo-initiator (PEGA200) and 2,2′-azobis(2-methyl-*N*-(2-hydroxyethyl)propionamide) (VA-086) was employed for the soap-free emulsion polymerization of styrene, the conductivity of aqueous phase where the soluble PSt chains ended with the initiator fragment exited exhibited an interesting tendency that the more hydrophobic initiators, AIBN and V-59, gave rise to much higher conductivity than the more hydrophilic PEG200 and V-068 [35]. For example, by using V-068, the conductivity was ca 4 μS/cm at 70 °C, whereas by using AIBN, it was about 25 μS/cm.

The conclusion was also applicable to explain the electric phenomena of random copolymer. Since the random distribution of solvophobic segments, the charge distribution along the copolymer chain was random. However, it is still unknown how to buildup the relationship between the orientational relaxation and the charges.

Of course, on the view of diblock copolymer itself, an explanation was also acceptable classically that the solvophobic block precipitated as a colloidal particle, which adsorbs the charges from the surrounding. In present paper, the positive charges were possibly supplied by MAA, namely that the solvophobic block adsorbed H^+ dissociated from –COOH. Scheme 1 shows the structure of diblock copolymer with a solvophobic block.

Nevertheless, the fact of charged diblock amphiphile indicated that the electrostatic interaction between the solvophobic blocks should be considered in the process of self-assembly. As shown in Scheme 1, the solvophobic blocks will not simply aggregate due to the so-called solvophobic interaction. The diblock copolymers look like micro-dipoles. If the self-assembly took place, the electrostatic interactions should

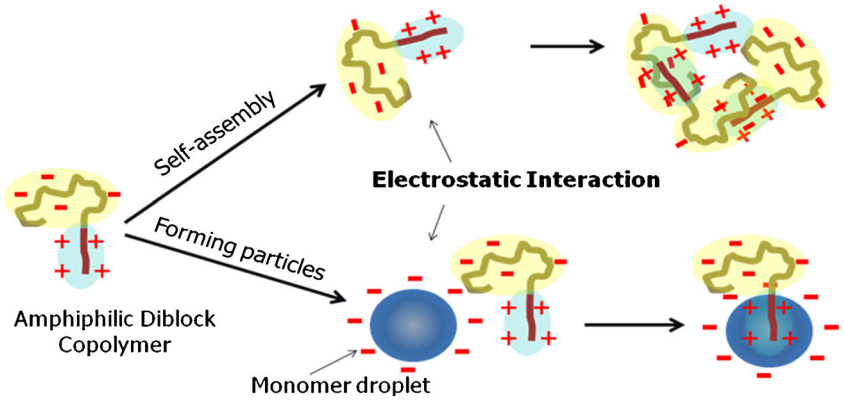

Scheme 1 Self-assembly and particle formation paths via amphiphilic diblock copolymers

play a negligible role. This may be the real reason that a tiny amount of ions, rather a large number, is indispensable in the self-assembly of diblock copolymers.

As for the particle formation, it was amazing that the charges of particles were opposite to the charges of soluble diblock copolymers. Especially the self-assembled P(MAA-b-St) (MAA/St=1/1) particles and P(MAA-b-4VP) particles were positive charged, though the content of MAA was dominant. Moreover, the diblock copolymers gave rise to the higher conductivity and simultaneously produced the particles, whereas the random copolymerization only produced the soluble copolymers. These results were hard to be explained by the conventional concepts of colloids, for instance, the collapse of dielectric double-layer [40] and the instability of nuclei [38]. And also, it was difficult to explain these results by employing the conventional mechanism that the solvophobic blocks aggregated to form the core, while the solvophilic block dissolved to form corona which stabilized the self-assembly micelles [22, 23].

An explanation was suggested in Scheme 1 on the basis of results in this paper. There are two paths forming the particles. One is the self-assembly of amphiphilic diblock copolymers. The diblock copolymers are macrodipoles, thus the electrostatic interactions of dipoles play a key role on the self-assembly. The distribution of charges on the surface of particles determines the electric behavior of particles. The other one is the polymerization in the monomer droplets. The charge nature of monomer droplets determines the electric behavior of particles.

Summary

Utilizing PMAA as the soluble component, three representative types of monomer, i.e., AAm, St, and 4VP, were selected for the random copolymerization and RAFT copolymerization. Among them, AAm is soluble in ethanol and interacts with both MAA and ethanol by hydrogen bonds, but PAAm is solvophobic. PSt is just solvophobic. Both 4VP and P4VP is soluble in ethanol, but they form the zwitterions with MAA. The above results clearly indicated that the soluble diblock copolymer amphiphile was quite different from the random copolymer. With respect to the electric property, the soluble diblock polymeric amphiphile such as poly(MAA-b-AAm) and poly(MAA-b-St) was positively charged and gave rise to high conductivity of solution, whereas the charges of random copolymers such as poly(MAA-co-St) and poly(MAA-co-4VP) were not detectable. For the formation of particles, the block copolymer such as poly(MAA-b-AAm), poly(MAA-b-4VP) were easily prepared, but it was hard to prepare by the random copolymers such as poly(MAA-co-4VP) and poly(MAA-co-St).

Acknowledgments The research was supported by Chinese National Fund for Science (NSFC, 51073035) and the International Corporation Project (201101088) with Science and Technology Bureau, Nanjing Municipal.

References

1. Tanner P, Baumann P, Enea R, Onaca O, Palivan C, Meier W (2011) Polymeric vesicles: from drug carriers to nanoreactors and artificial organelles. Acc Chem Res 44:1039–1049
2. Pai RA, Humayun R, Schulberg MT, Sengupta A, Sun JN, Watkins JJ (2004) Mesoporous silicates prepared using preorganized templates in supercritical fluids. Science 303:507–510
3. Hayward RC, Chmelka BF, Kramer EJ (2005) Crosslinked poly (styrene)-block-poly(2-vinylpyridine) thin films as swellable templates for mesostructured silica and titania. Adv Mater 17:2591–2595
4. Yuan JJ, Mykhaylyk OO, Ryan AJ, Armes SP (2007) Cross-linking of cationic block copolymer micelles by silica deposition. J Am Chem Soc 129:1717–1723
5. Wang CW, Sinton D, Moffitt MG (2011) Flow-directed block copolymer micelle morphologies via microfluidic self-assembly. J Am Chem Soc 133:18853–18864
6. Hayward RC, Pochan DJ (2010) Tailored assemblies of block copolymers in solution: it is all about the process. Macromolecules 43:3577–3584
7. Cui H, Chen Z, Zhong S, Wooley KL (2007) Block copolymer assembly via kinetic control. Science 317:647–650
8. Blanazs A, Massignani M, Battaglia G, Armes SP (2009) Tailoring macromolecular expression at polymersome surfaces. Adv Funct Mater 19:2906–2914
9. Ni HM, Wu M, Li M, Wang HL, Sun YM (2010) Quasi-static particle formation of poly(acrylamide/methacrylic acid) in ethanol by using v-65 as initiator. Polym Chem 1:899–907
10. Ni HM, Du YZ, Ma GH, Nagai M, Omi S (2001) Mechanism of soap-free emulsion polymerization of styrene and 4-vinylpyridine: characteristics of reaction in the monomer phase, aqueous phase, and their interface. Macromolecules 34:6577–6585
11. Wan WM, Pan CY (2010) Formation of polymeric yolk/shell nanomaterial by polymerization-induced self-assembly and reorganization. Macromolecules 43:2672–2675
12. Zehm D, Ratcliffe LPD, Armes SP (2013) Synthesis of diblock copolymer nanoparticles via raft alcoholic dispersion polymerization: effect of block copolymer composition, molecular weight, copolymer concentration, and solvent type on the final particle morphology. Macromolecules 46:128–139
13. Sugihara S, Blanazs A, Armes SP, Ryan AJ, Lewis AL (2011) Aqueous dispersion polymerization: a new paradigm for in situ block copolymer self-assembly in concentrated solution. J Am Chem Soc 133:15707–15713
14. Zhang X, Rieger J, Charleux B (2012) Effect of the solvent composition on the morphology of nano-objects synthesized via RAFT polymerization of benzyl methacrylate in dispersed systems. Polym Chem 3:1502–1509
15. Boisse S, Rieger J, Belal K, Beaunier P, Li MH, Charleux B (2010) Amphiphilic block copolymer nano-fibers via RAFT-mediated polymerization in aqueous dispersed system. Chem Commun 46:1950–1952
16. Rieger J, Zhang W, Stoffelbach F, Charleux B (2010) Surfactant-free RAFT emulsion polymerization using poly(N, N-dimethylacrylamide) trithiocarbonate macromolecular chain transfer agents. Macromolecules 43:6302–6310

17. Wan WM, Pan CY (2010) One-pot synthesis of polymeric nanomaterials via RAFT dispersion polymerization induced self-assembly and re-organization. Polym Chem 1:1475–1484
18. Wan WM, Sun XL, Pan CY (2010) Formation of vesicular morphologies via polymerization induced self-assembly and re-organization. Macromol Rapid Commun 31:399–404
19. Ratclie LPD, Ryan AJ, Armes SP (2013) From a water-immiscible monomer to block copolymer nano-objects via a one-pot RAFT aqueous dispersion polymerization formulation. Macromolecules 46:769–777
20. Fielding LA, Derry MJ, Ladmiral V, Rosselgong J (2013) RAFT dispersion polymerization in non-polar solvents: facile production of block copolymer spheres, worms and vesicles in n-alkanes. Chem Sci 4:2081–2087
21. Ahmed R, Patra SK, Hamley IW, Manners I, Faul CFJ (2013) Tetragonal and helical morphologies from polyferrocenylsilane block polyelectrolytes via ionic self-assembly. J Am Chem Soc 135:2455–2458
22. Borisov OV, Zhulina EB (2013) Theory of self-assembly of triblock ter-polymers in selective solvent towards corona-compartmentalized (Janus) micelles. Polymer 54:2043–2048
23. Zhulina EB, Borisov OV (2012) Theory of block polymer micelles: recent advances and current challenges. Macromolecules 45:4429–4440
24. Ni HM, Ma GH, Nagai M, Omi S (2001) Effects of ethyl acetate on the soap-free emulsion polymerization of 4-vinylpyridine and styrene. I. Aspects of the mechanism. J Appl Polym Sci 82:2679–2691
25. Ni HM, Kawaguchi H (2004) Mechanism of preparing monodisperse poly(acrylamide/ methacrylic acid) microspheres in ethanol. J Polym Sci A Polym Chem 42:2823–2833
26. Ni HM, Kawaguchi H, Endo T (2007) Preparation of pH-sensitive hydrogel microspheres of poly (acrylamide-co-methacrylic acid) with sharp pH-volume transition. Colloid Polym Sci 285:819–826
27. Ni HM, Kawaguchi H, Endo T (2007) Preparation of amphoteric microgels of poly(acrylamide/methacrylic acid/dimethylamino ethylene methacrylate) with a novel ph-volume transition. Macromolecules 40:6370–6376
28. Tanaka T, Komatsu Y, Fujibayashi T, Minami H, Okubo M (2010) A novel approach for preparation of micrometer-sized, monodisperse dimple and hemispherical polystyrene particle. Langmuir 26:3848–3853
29. Ni HM, Ma GH, Nagai M, Omi S (2001) Effects of ethyl acetate on the soap-free emulsion polymerization of 4-vinylpyridine and styrene. II. Aspects of the mechanism. J Appl Polym Sci 82:2692–2708
30. Ni HM, Ma GH, Nagai M, Omi S (2001) Novel method of preparation of a charged mosaic membrane by using dipole-like microspheres. II. Preparation of dumbbell/egg-like microspheres. J Appl Polym Sci 80:2002–2017
31. Minami H, Kobayashi H, Okubo M (2005) Preparation of hollow polymer particles with a single hole in the shell by SaPSeP. Langmuir 21:5655–5658
32. Takekoh R, Li WH, Burke NAD, Stover HDH (2006) Multilayered polymer microspheres by thermal imprinting during microsphere growth. J Am Chem Soc 128:240–244
33. Fujibayashi T, Okubo M (2007) Preparation and thermodynamic stability of micron-sized, monodisperse composite polymer particles of disc-like shapes by seeded dispersion polymerization. Langmuir 23:7958–7962
34. Ahmad F, Baloch MK, Jamil M, Jeon YJ (2010) Characterization of polystyrene-b-poly(ethylene oxide) diblock copolymer and investigation of its micellization behavior in water. J Appl Polym Sci 118:1704–1712
35. Tauer K, Hernandez H, Kozempel S, Lazareva O, Nazaran P (2008) Towards a consistent mechanism of emulsion polymerization-new experimental details. Colloid Polym Sci 286:499–515
36. Li M, Ni HM (2011) Conductimetry study of the precipitation polymerization of acrylamide and methacrylic acid in ethanol by using V-65 as initiator. Intl Conf Remote Sens Environ Transp Eng 455:6707–6710
37. Li M, Ni HM (2012) Study on the precipitation polymerization of acrylamide and methacrylic acid in ethanol by conductimetry: phase-separation prior to polymerization. Adv Mater Res 455–456:639–644
38. Fitch RM (1997) In Polymer colloids: a comprehensive introduction. Academic Press, New York, Chapter 3
39. Fayer MD (2012) Dynamics of water interacting with interfaces, molecules, and ions. Acc Chem Res 45:3–14
40. Ni HM, Ma GH, Nagai M, Omi S (2001) Effects of ethyl acetate on the soap-free emulsion polymerization of 4-vinylpyridine and styrene. J Appl Polym Sci 80:1988–2001